School of Engineering and Digital Sciences
Department of Chemical & Materials Engineering
Nazarbayev University

# ROS mediated theranostic materials

Supervisor: Chang-Keun Lim
Co-Supervisor: Dhawal Shah

Ayaulym Abilova
201518438

# Background: Reactive Oxygen Species (ROS)

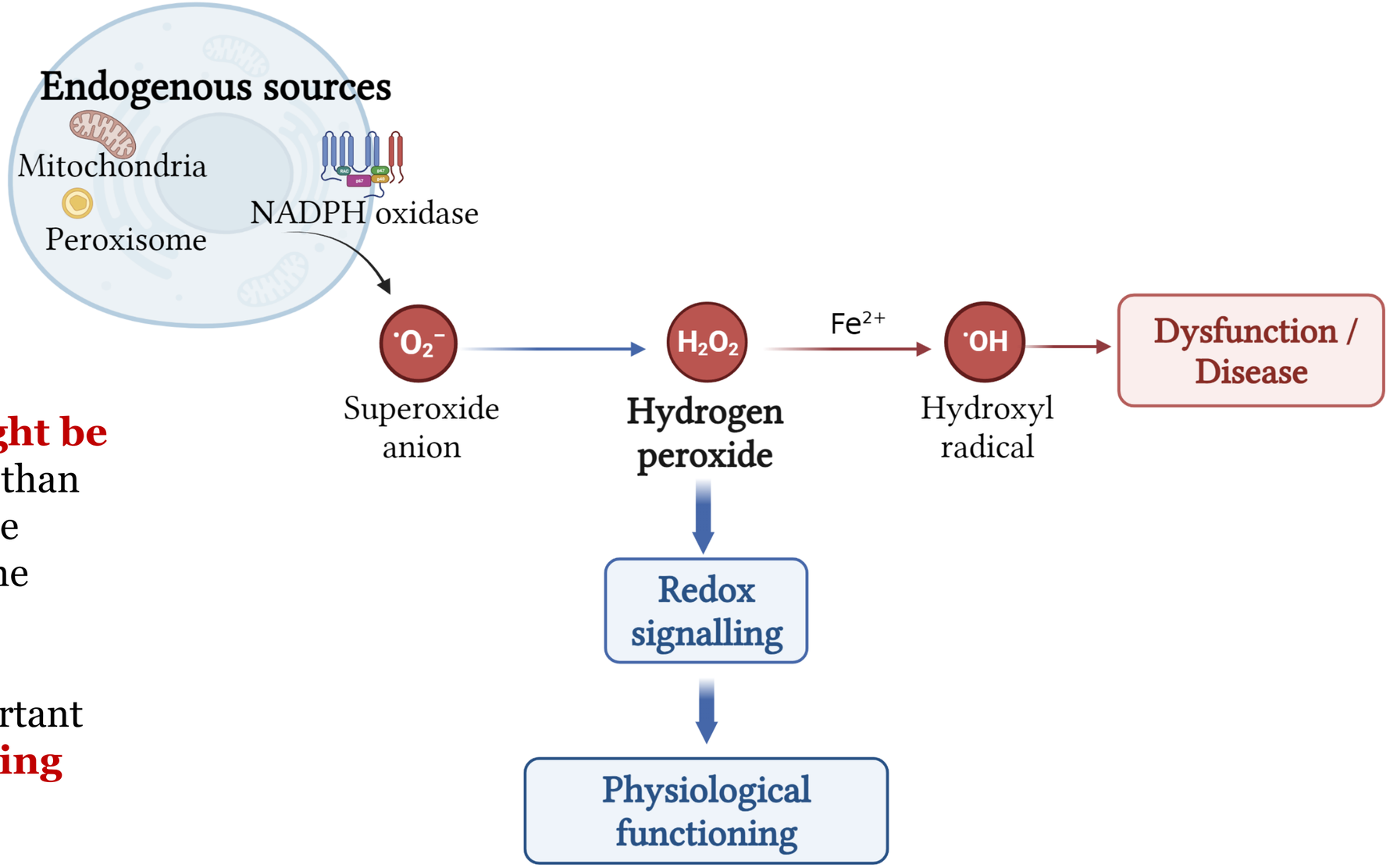


**Hydrogen peroxide contents in tumors might be up to 100 times higher** than in normal tissues due to the abnormal metabolism of the cancer cells.

Therefore, ROS is an important **biomarker for bioimaging and drug delivery**.

# Background: Visualization of ROS

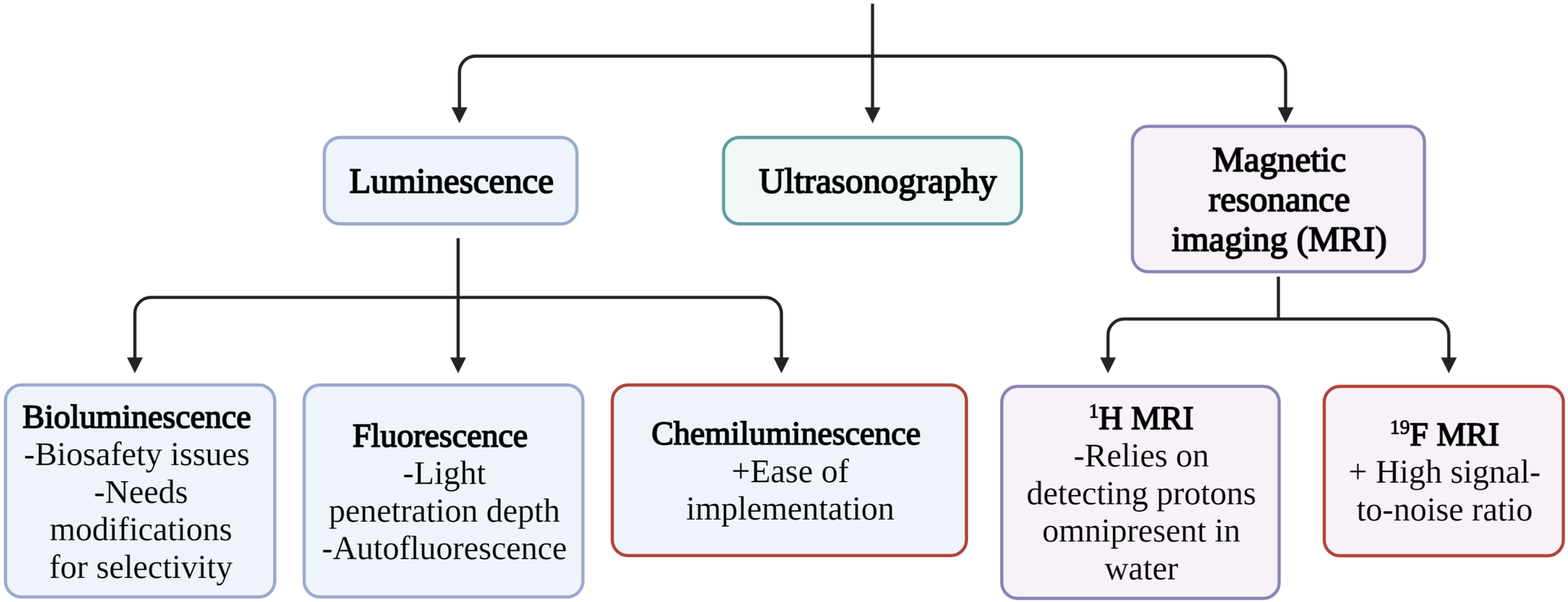

# Background: Switching $^{19}$F MRI imaging

Restricted mobility of the fluorinated segments within the core
=> **shorter $T_2$** relaxation time
=> **attenuated $^{19}$F MRI signal**

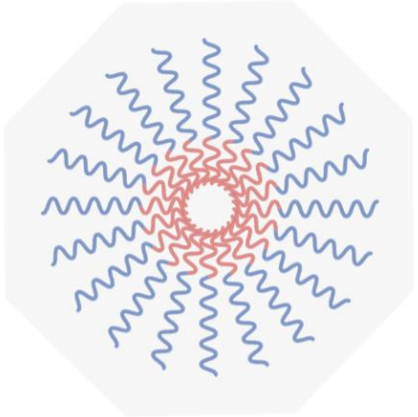

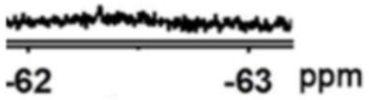


$^{19}$F MRI 'off'

Disassembly

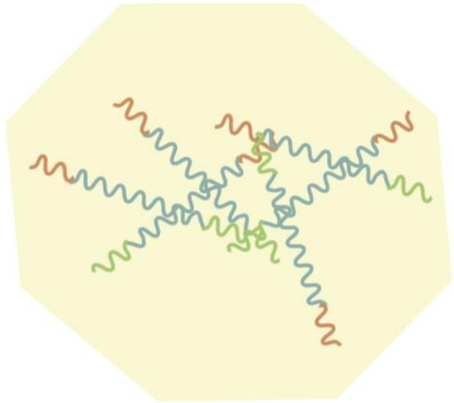

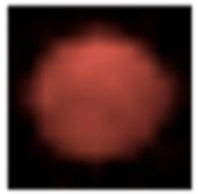

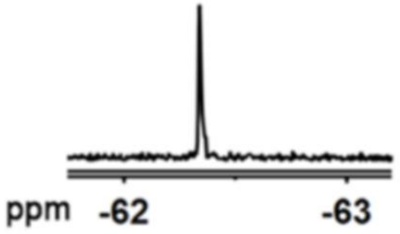


$^{19}$F MRI 'on'

Disassembly of the aggregated nanoparticles
=> **longer $T_2$** relaxation time
=> **enhanced $^{19}$F MRI signal**

Li, A., Luo, X., Li, L., Chen, D., Liu, X., Yang, Z., Yang, L., Gao, J., & Lin, H. (2021). Activatable multiplexed $^{19}$F magnetic resonance imaging visualizes reactive oxygen and nitrogen species in drug-induced acute kidney injury. *Analytical Chemistry*, *93*(49), 16552–16561. https://doi.org/10.1021/acs.analchem.1c03744

# Background: Peroxyoxalate chemiluminescence

- Schaap's dioxetane-based systems
- Donor-acceptor-donor structures
- Peroxyoxalate-based systems

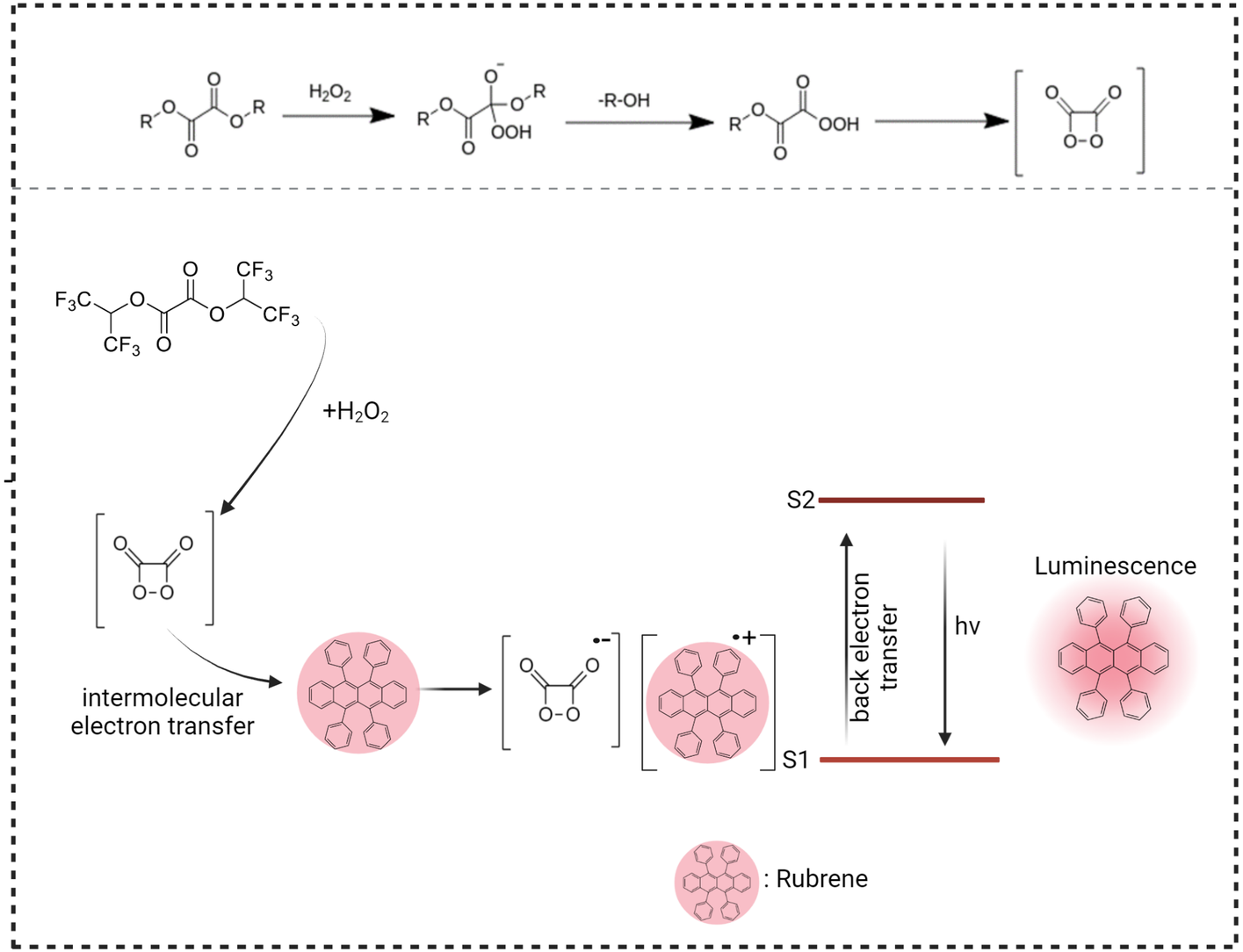

# Background: Aims

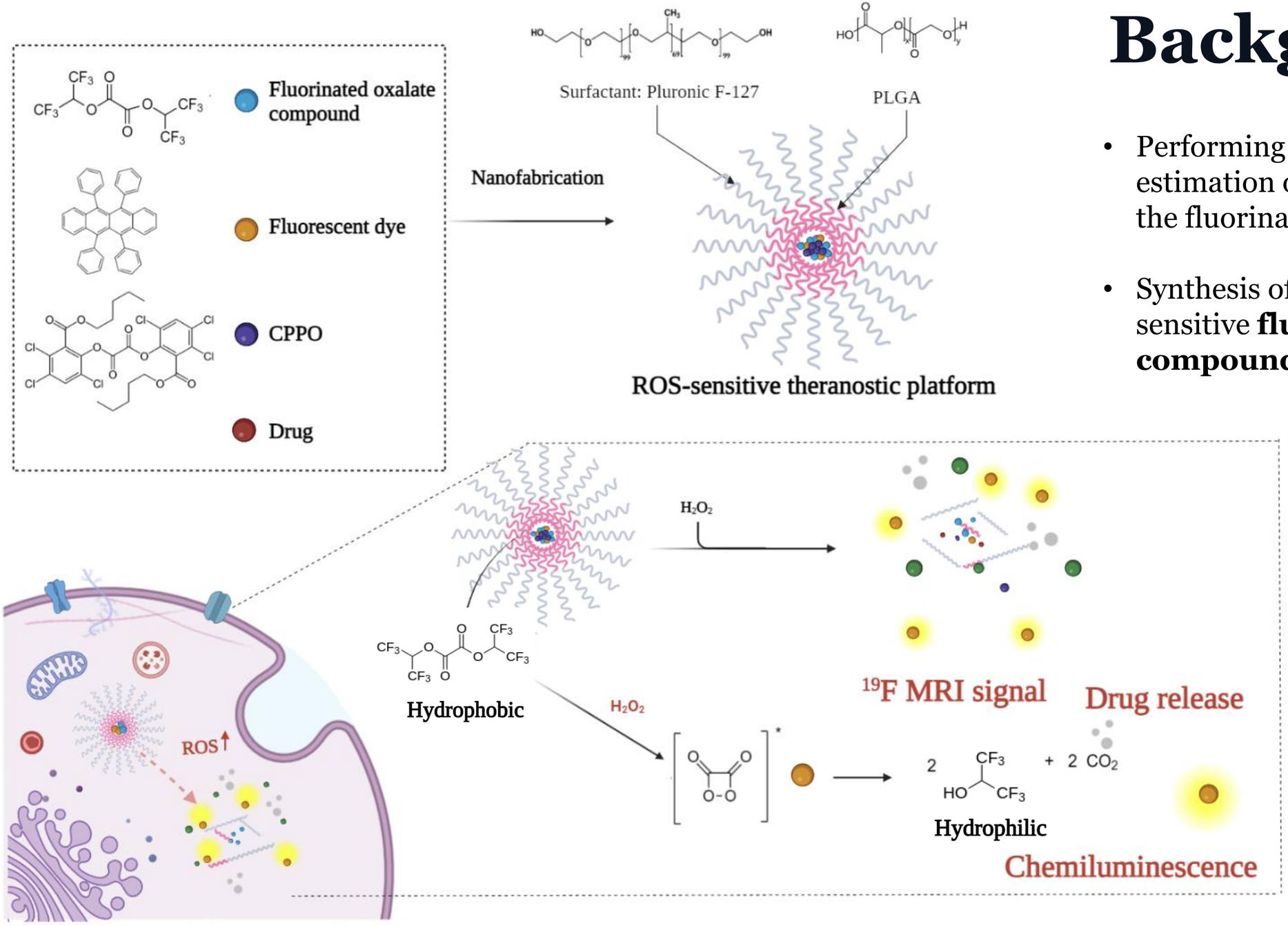


Schematic illustration ROS mediated theranostic nanoparticles.

- Performing **DFT calculations** for the estimation of the reactivity and stability of the fluorinated oxalate compound.
- Synthesis of the hydrogen peroxide-sensitive **fluorinated oxalate compound (FOC)**.
- Engineering reactive oxygen species-mediated **theranostic nanocarriers** to realize:

  - Chemiluminescence imaging;
  - $^{19}$F MRI contrast;
  - ROS-stimulated drug delivery.

# Methods

## DFT calculations

Geometry optimizations were performed in Gaussian 16 and GausView 6.0.16 software using B3LYP/6-31G or Def2DVP basis sets.

## FOC synthesis

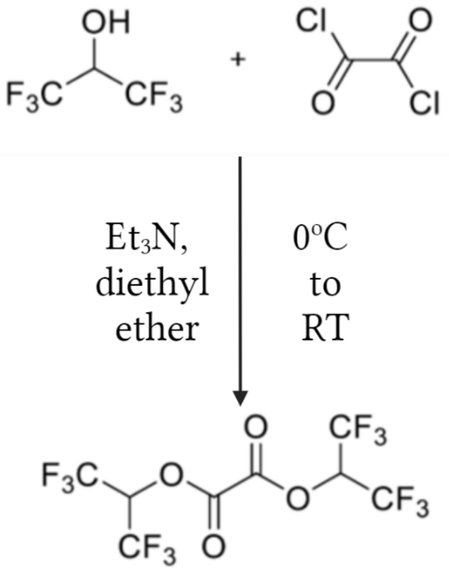


## Preparation of Nanoparticle

Rubrene - 0.04 mg
FOC - 2 mg
CPPO - 2 mg
PLGA - 0.4 mg
*dissolved in 500 µL DCM.*

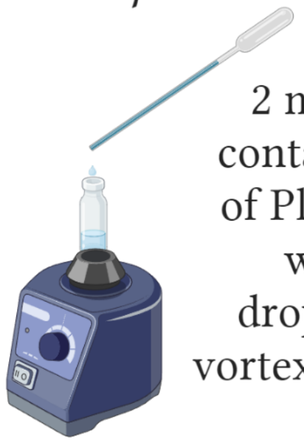

2 mL of water containing 40 mg of Pluronic F-127 was added dropwise while vortexing for 2 min.

DCM was evaporated using rotavapor at 300 mbar.

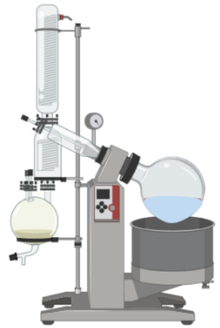

## Characterization of Nanoparticles

- DLS;
- TEM;
- *In vitro* Cytotoxicity Test;

### Chemiluminescence

IVIS → ROS imaging

PL → CL spectrum

### *In vitro* drug release

Photoluminescence of MRC-5 cells incubated with NPs loaded with PpIX (PDT drug)

### Demonstration of $^{19}$F MRI imaging → $^{19}$F NMR

# Results: Electrostatic potential surface.


**FOC**

ESP surface value: 0.04

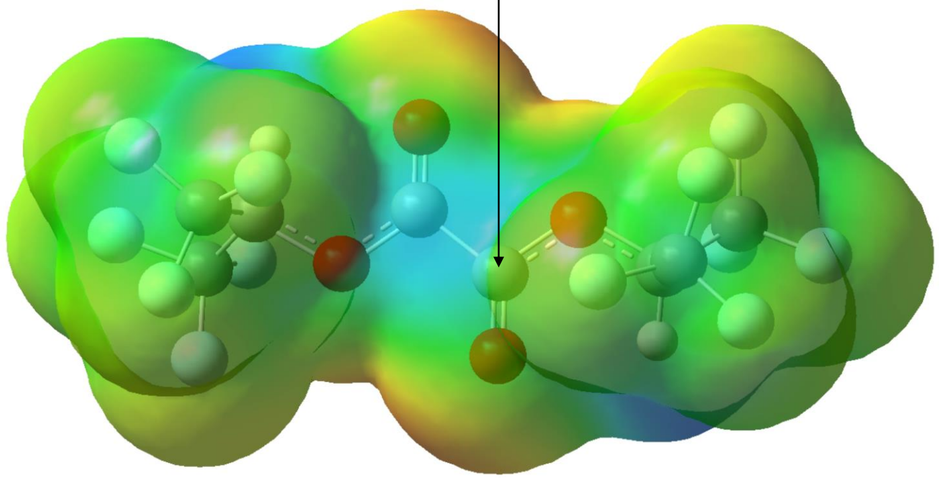

**CPPO**

ESP surface value: 0.0028

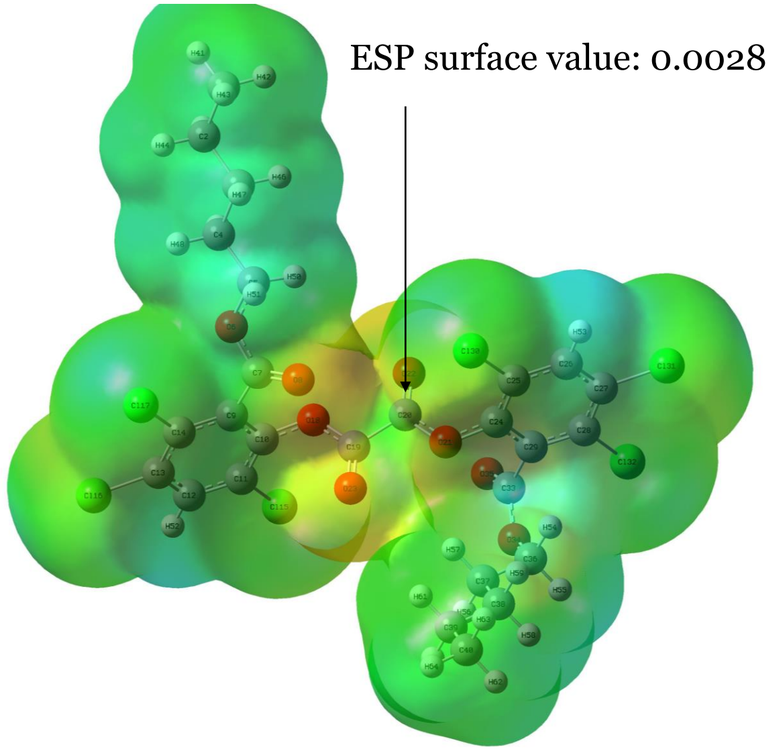

❖ **Carbonyl group in FOC is highly electro-deficient for efficient nucleophilic attack.**

# Results: DFT calculations

Total energy for the reaction of FOC and CPPO with hydrogen peroxide.

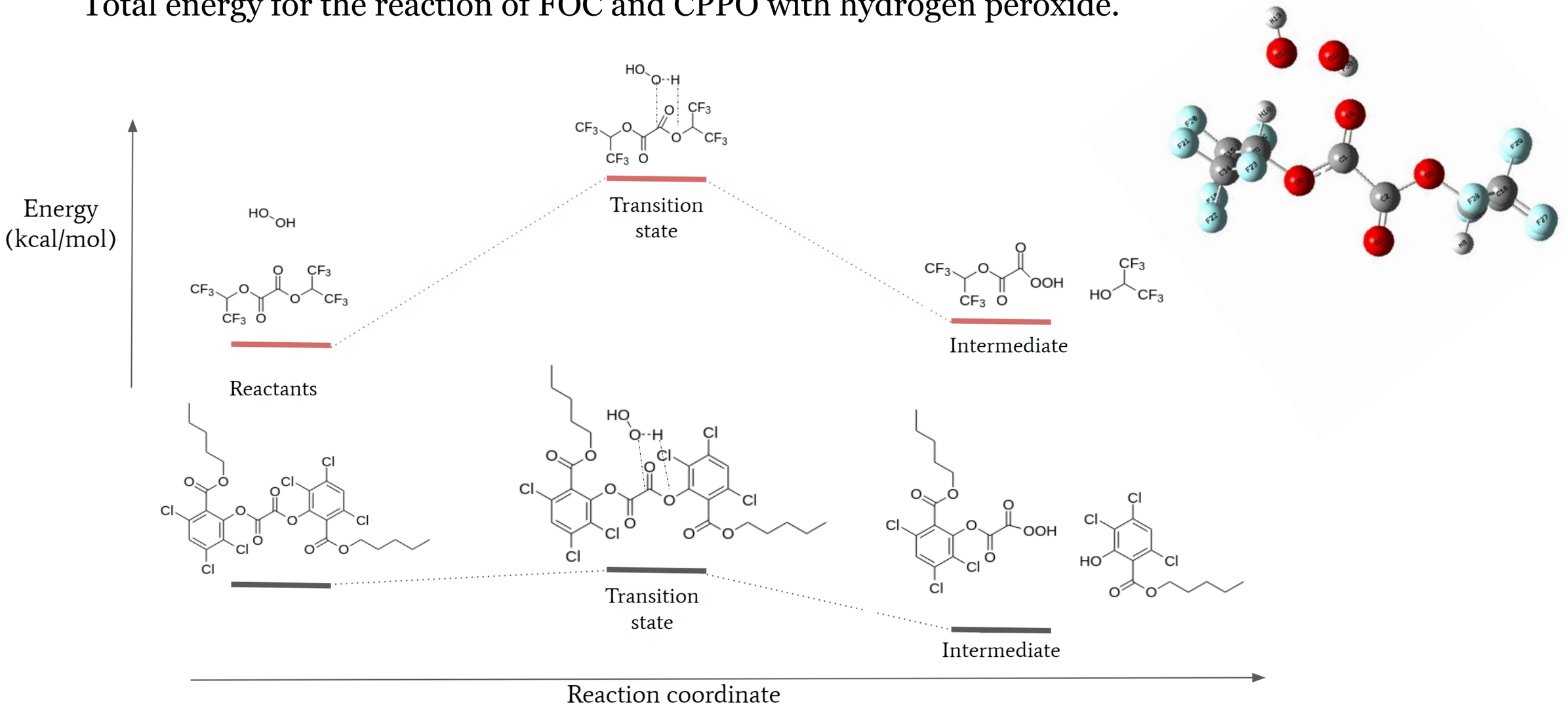




❖ **However, the activation energy of perhydrolysis of FOC is higher than CPPO, which is well correlated with experimental results.**

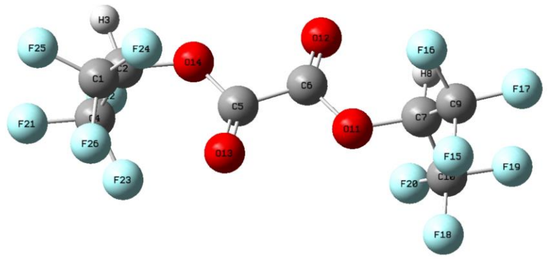

# Results: Synthesis of FOC


$^{1}$H NMR spectra

$^{13}$C NMR spectra

$^{19}$F NMR spectra

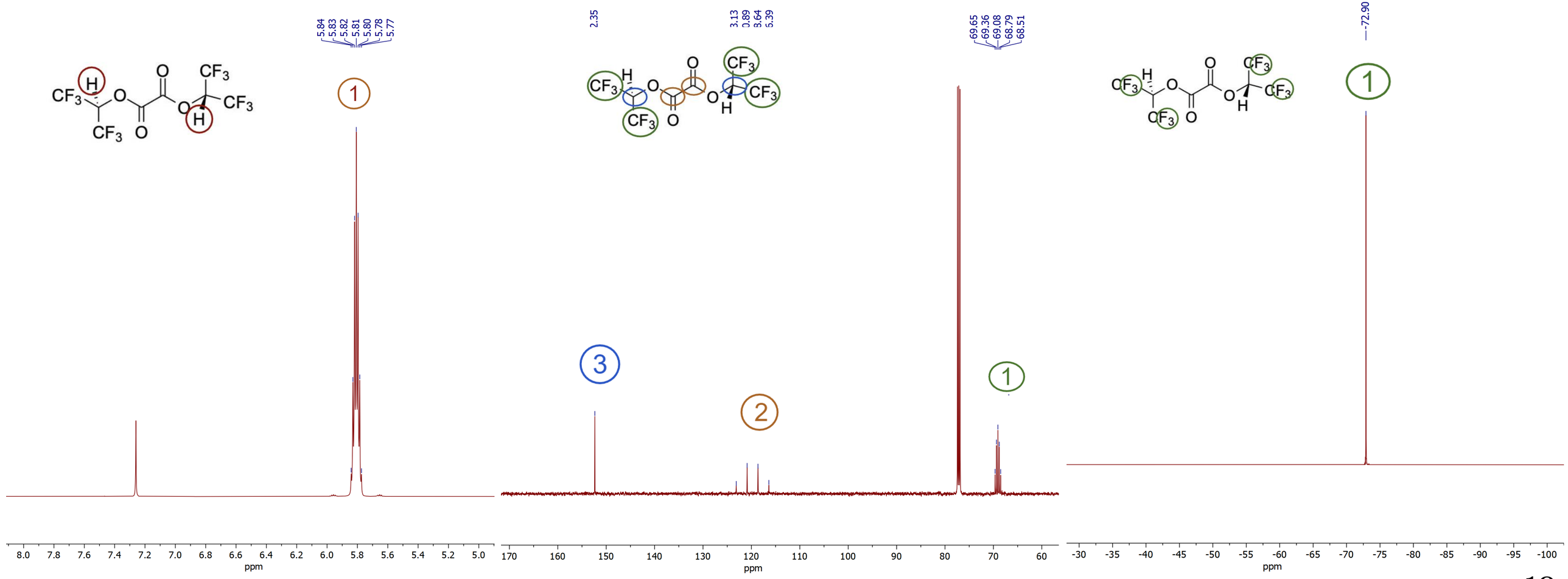

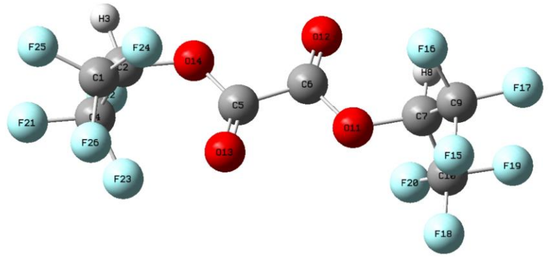

# Results: Chemiluminescence of FOC-Rubrene

Chemiluminescence spectra of 10 mg FOC and 0.2 mg Rubrene after the addition of 1 M $H_2O_2$ in THF.

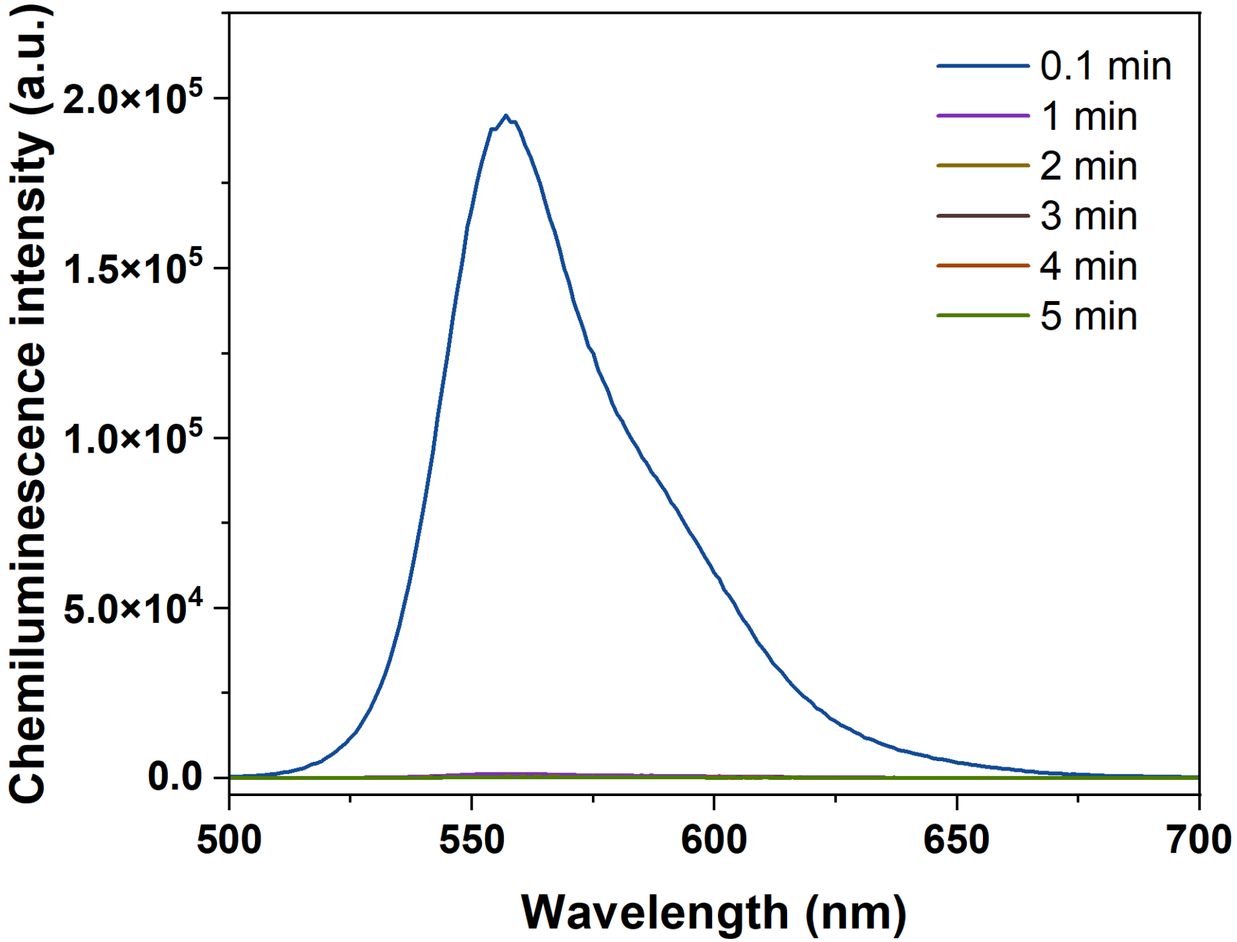


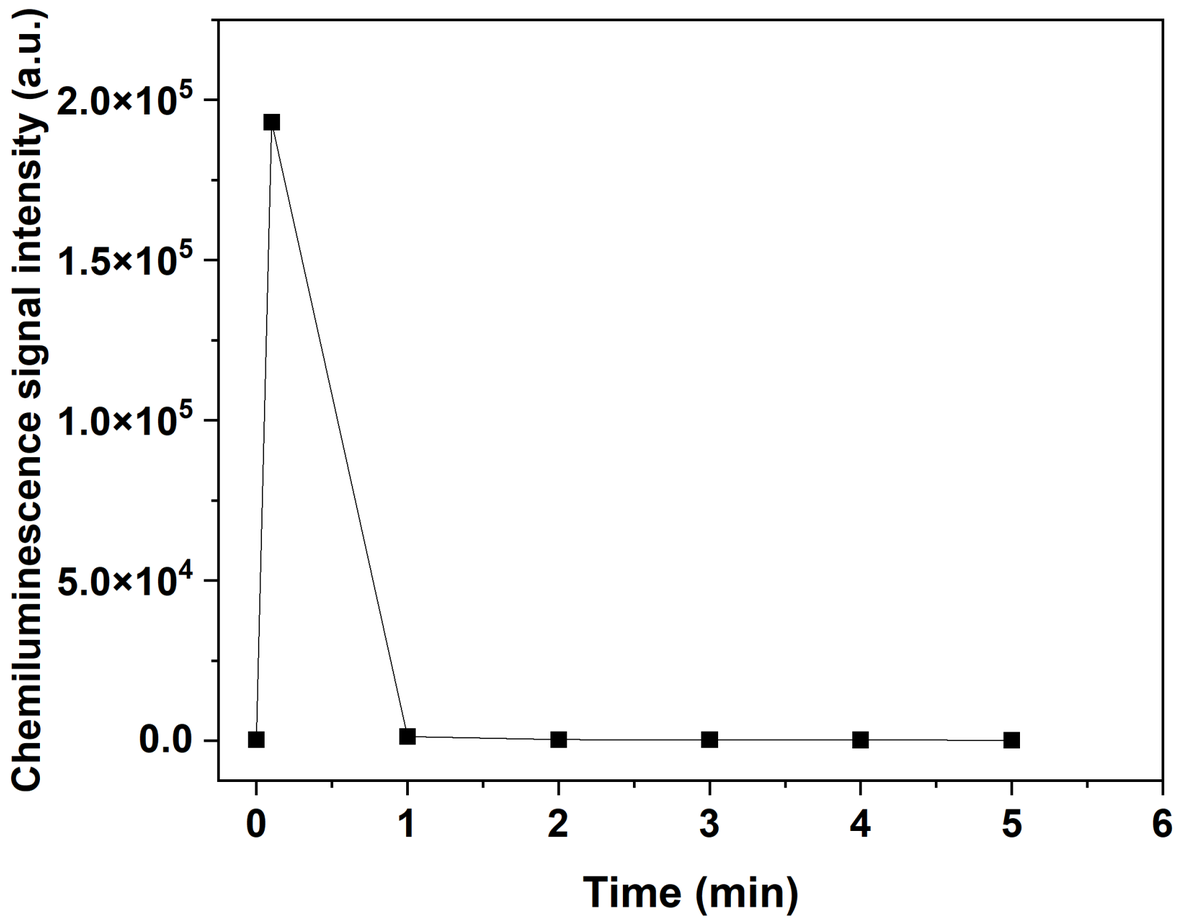

# Results: Characterization of Nanoparticles

TEM image of nanoparticles

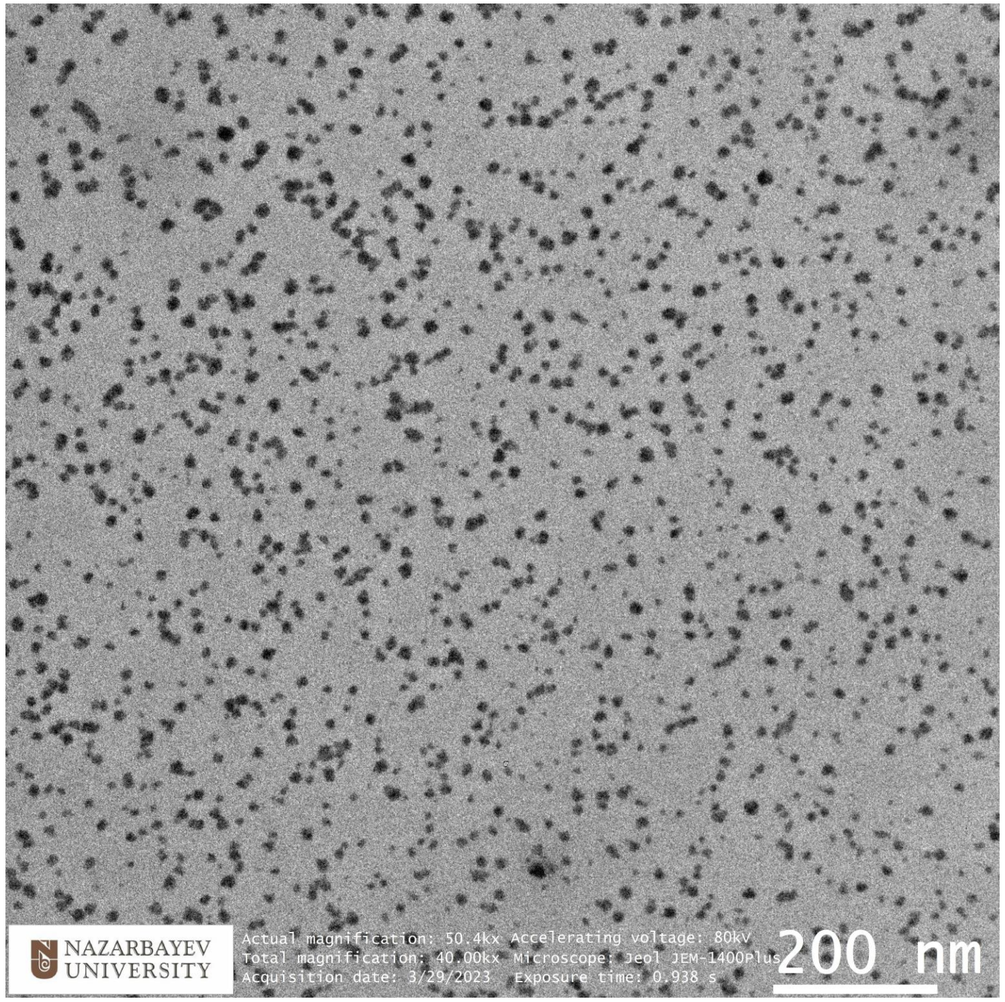


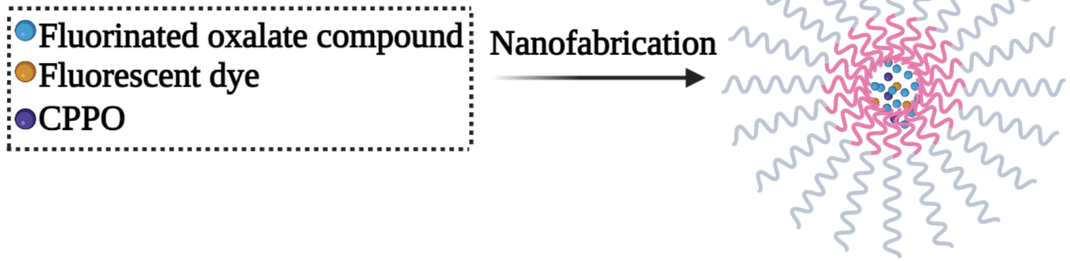


Dynamic light scattering size distribution

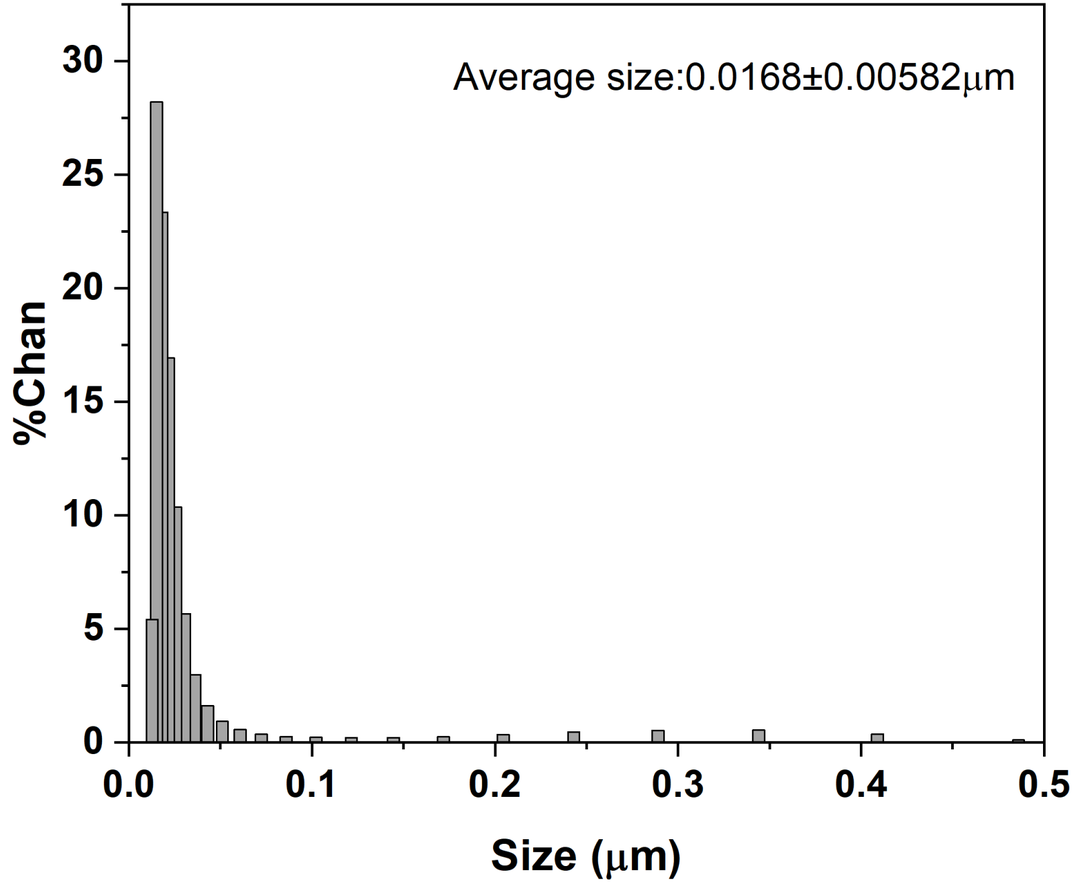

# Results: ROS-induced Degradation of Nanoparticle

Dynamic light scattering results after adding hydrogen peroxide

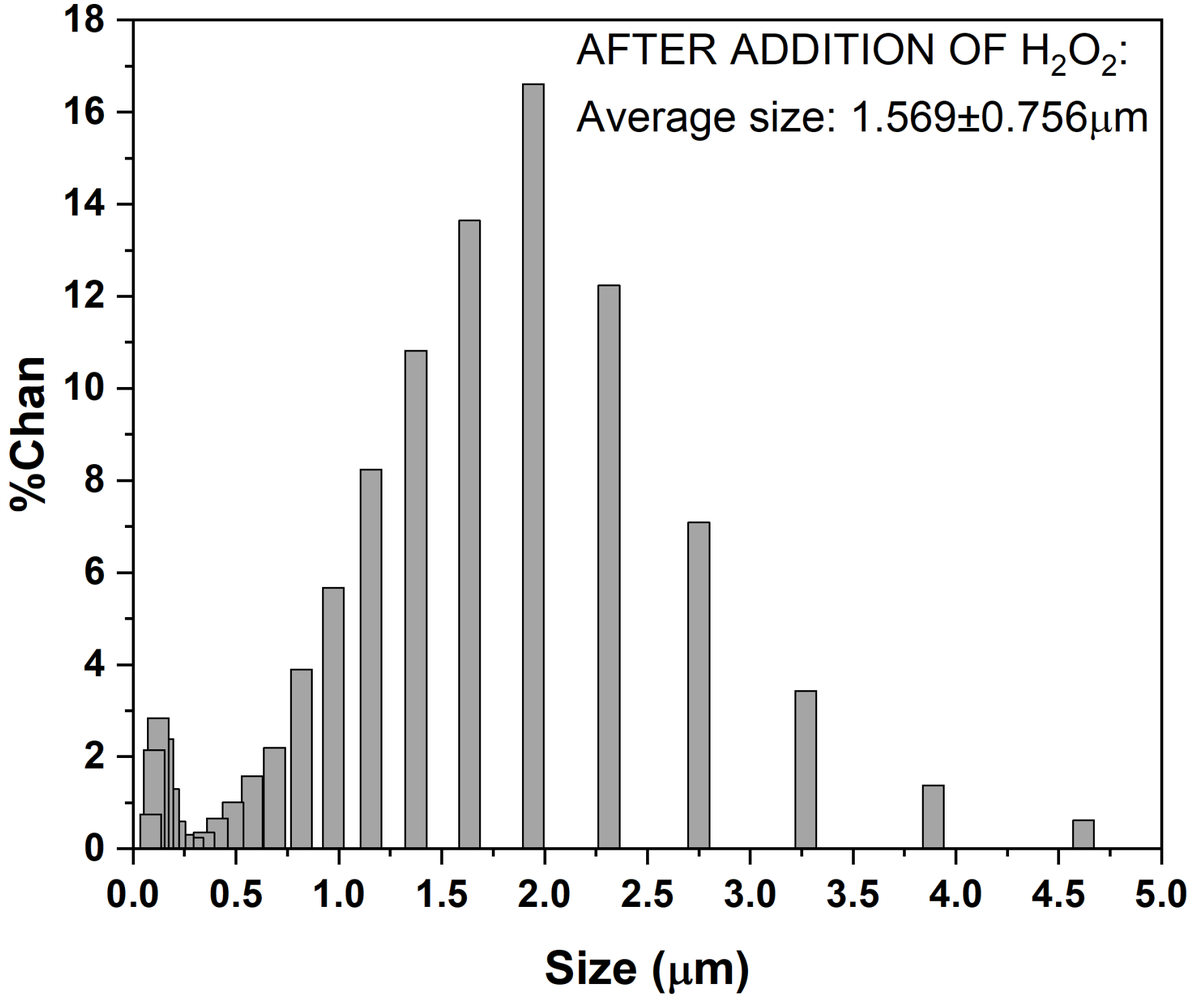


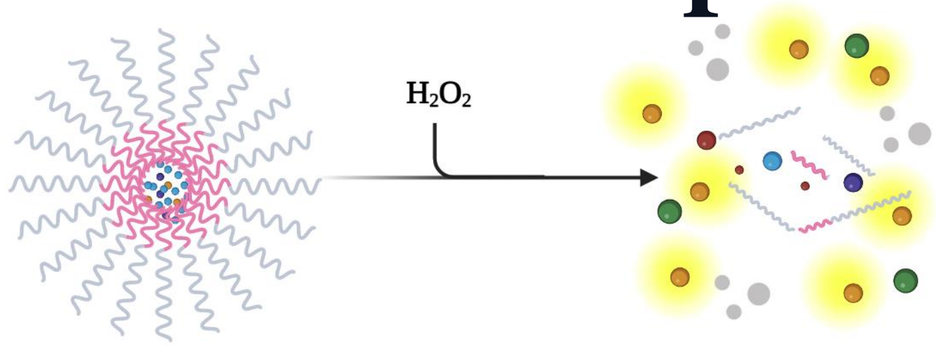


Average size ± standard error before and after adding hydrogen peroxide

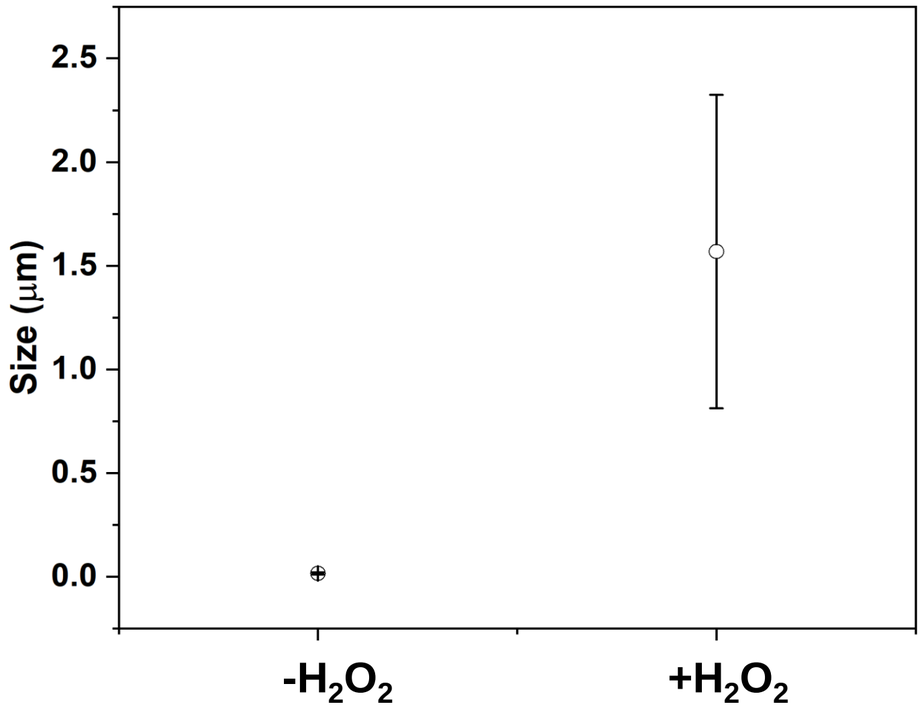


❖ **Successful demonstration of ROS triggered particle degradation.**

# Results: $^{19}$F NMR spectra of nanoparticles

The ratiometric signal intensity of $^{19}$F NMR spectra of nanoparticles before and after the addition of hydrogen peroxide. “Turn off” and “turn on” signals for FOC and 1,1,1,3,3,3-hexafluoro-2-propanol.

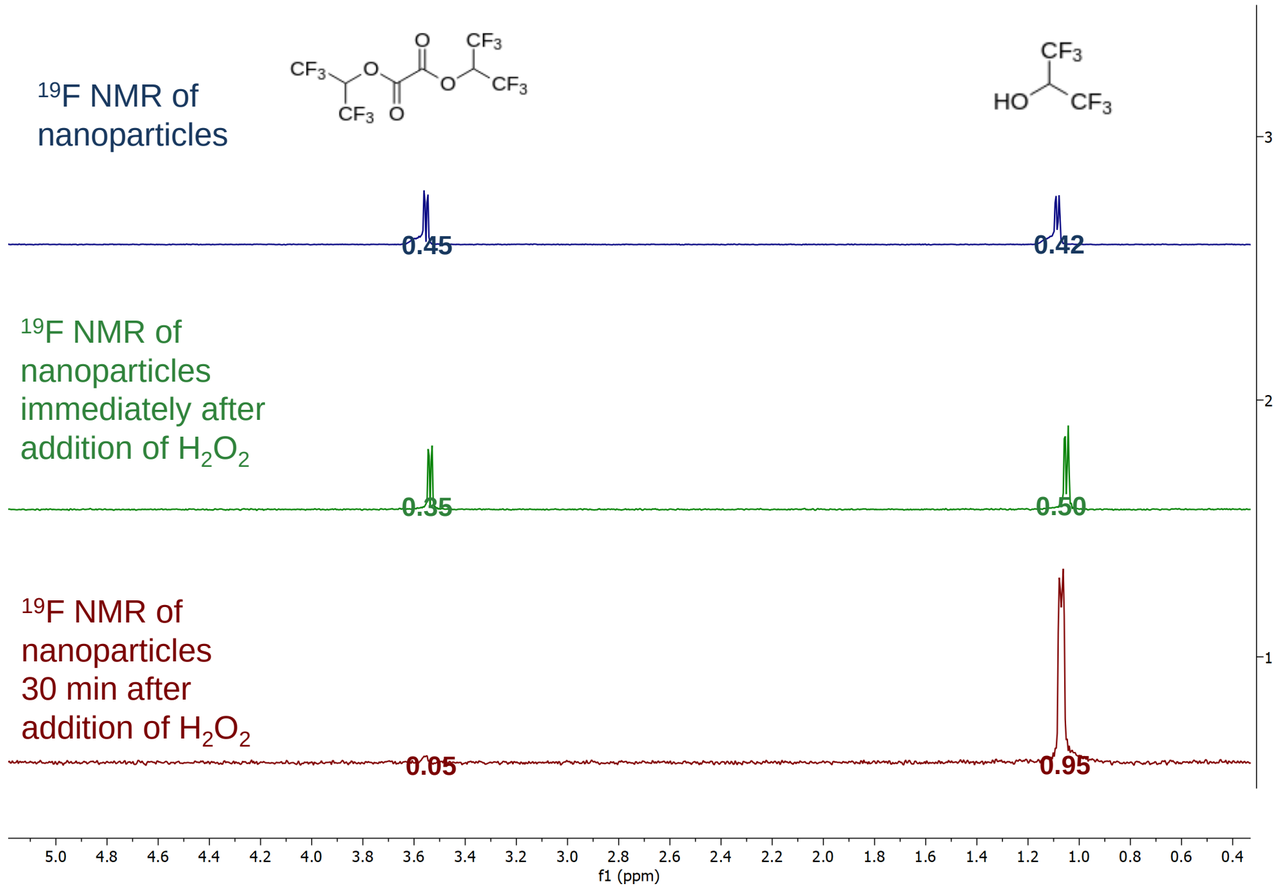


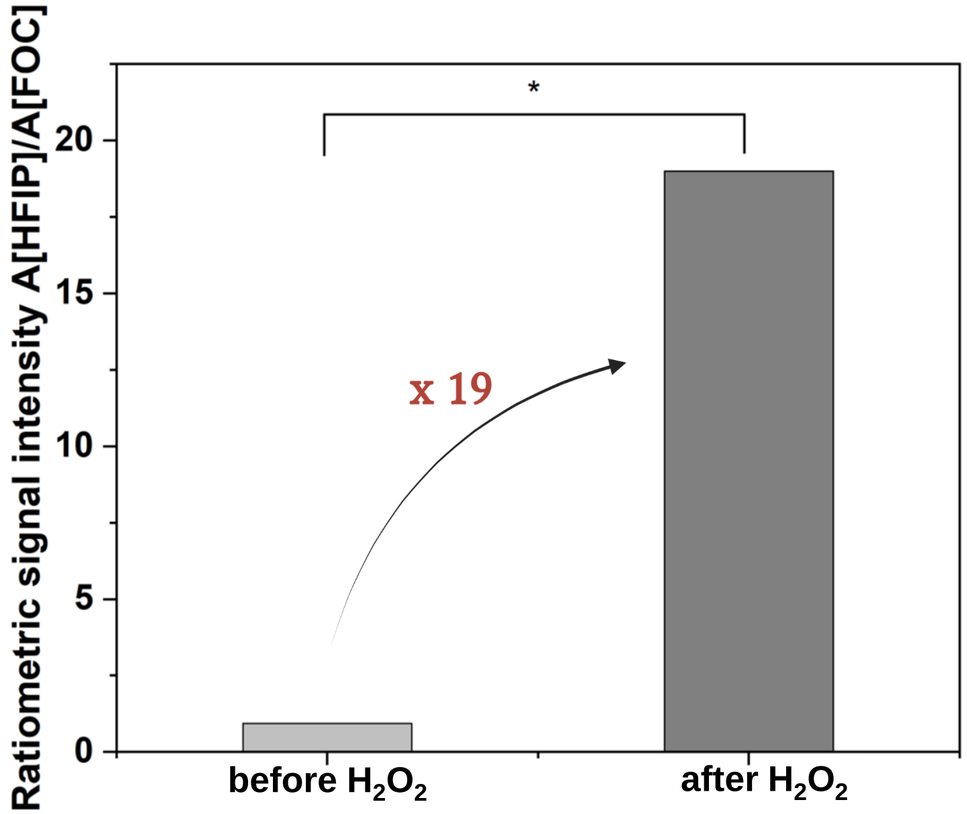


❖ **Promising contrast for $^{19}$F MRI imaging application.**

# Results: Chemiluminescence spectra of nanoparticles

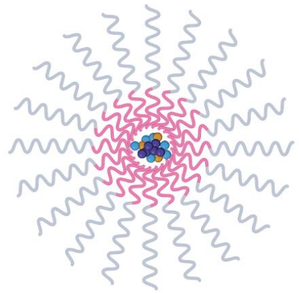

Chemiluminescence spectra of the nanoparticles with time.

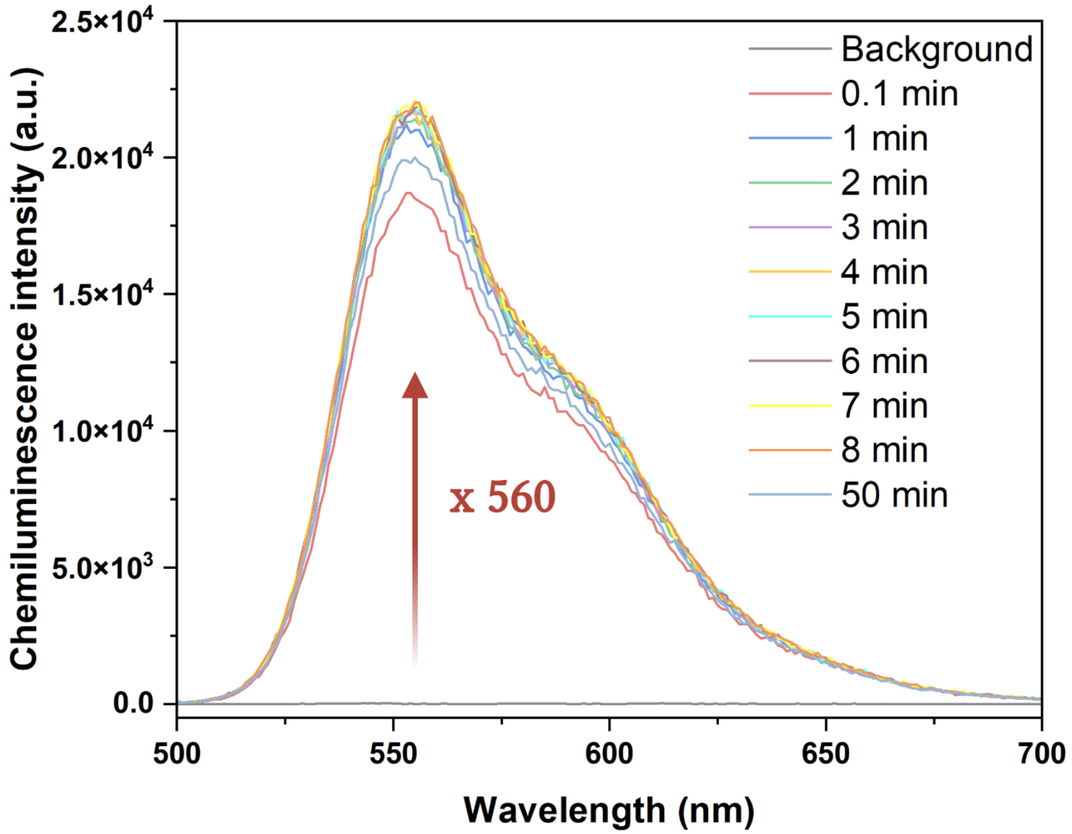


Chemiluminescence of the nanoparticles at $10^{-5}$ M hydrogen peroxide visualized and quantified using IVIS Spectrum CT.

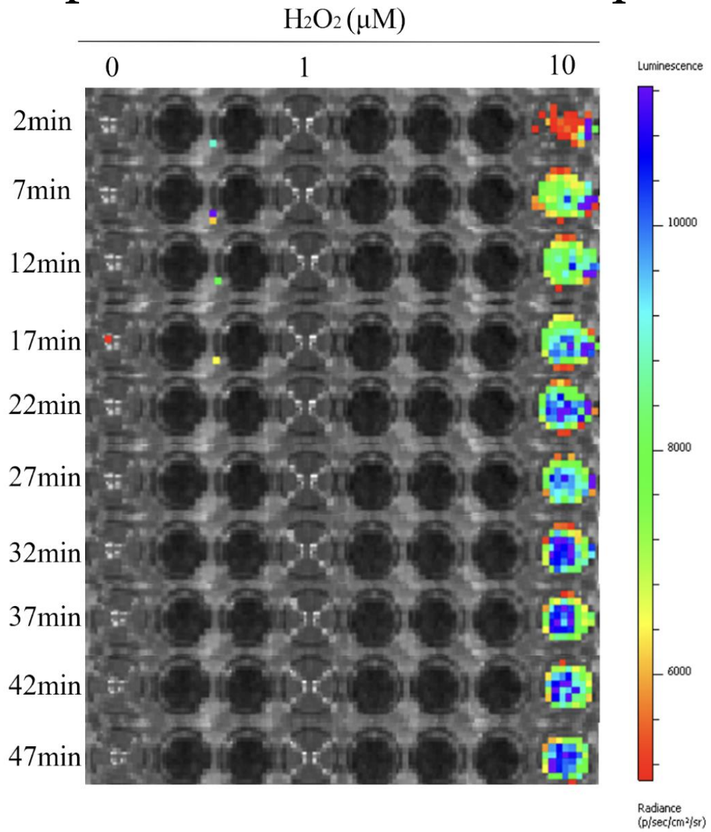


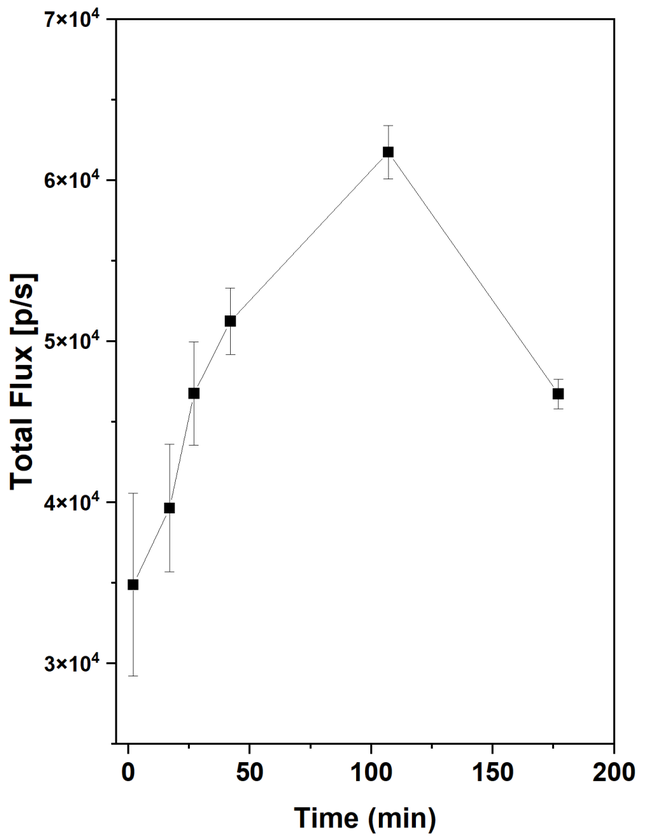


❖ **Promising contrast for CL imaging application.**

# Results: *In vitro* Material Toxicity

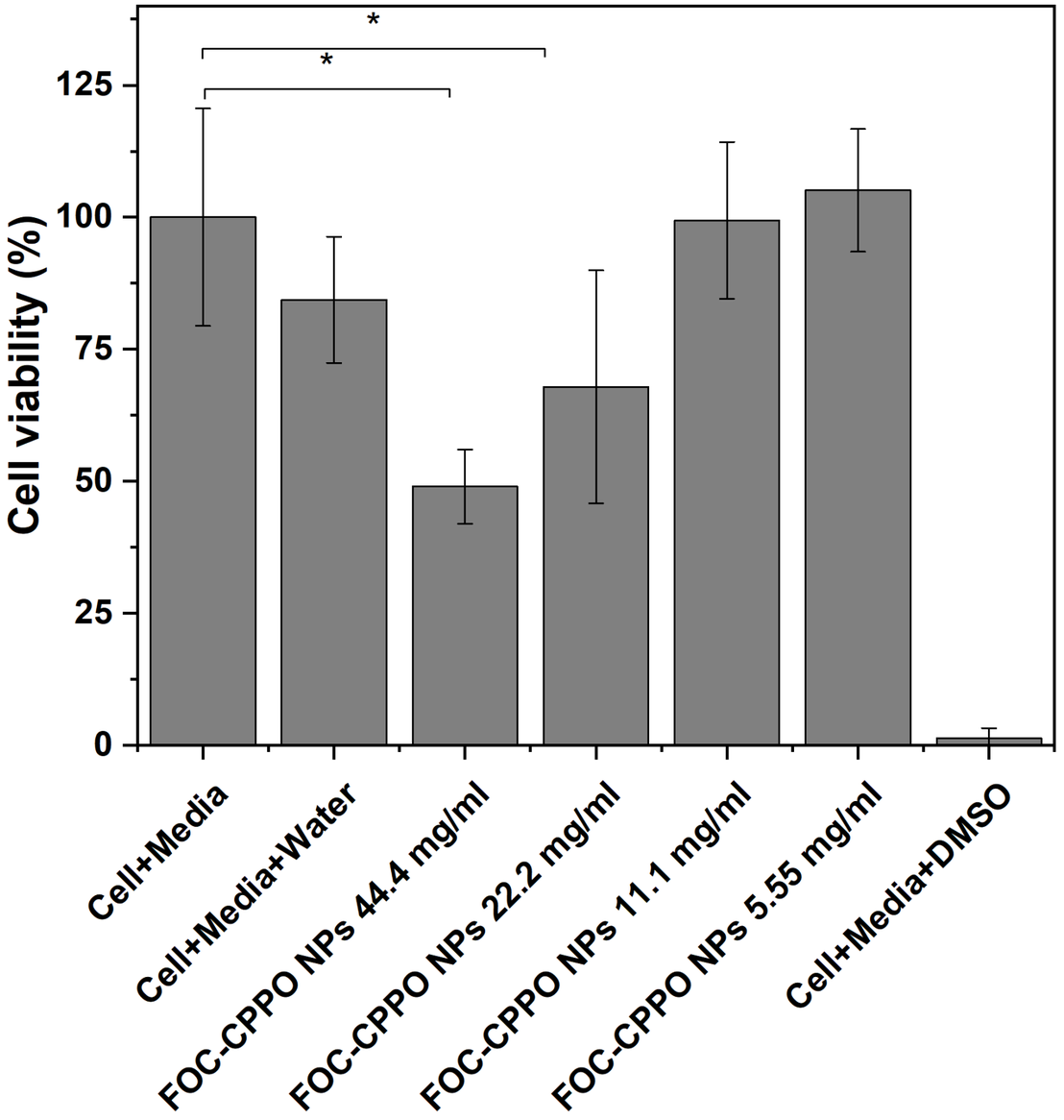


Cell viability falls below 50% at concentration 44.4 mg/ml.

11.1 mg/ml material toxicity is almost negligible.

- **Concentration – dependent toxicity of the material was observed.**

# Results: ROS-Responsive Drug Release

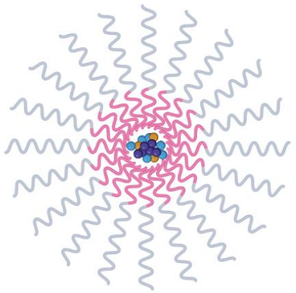

ROS triggered PpIX drug release from nanoparticles

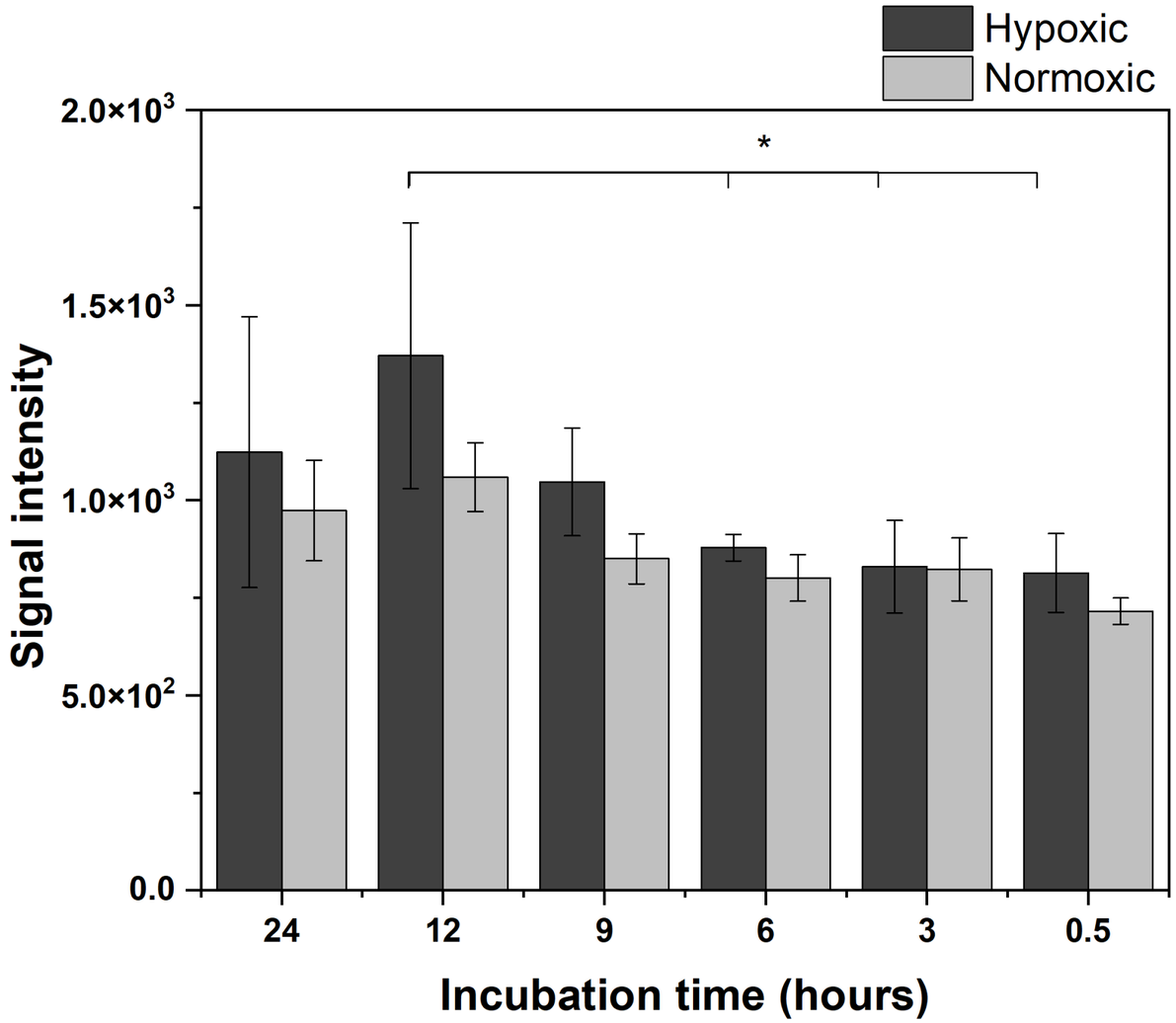


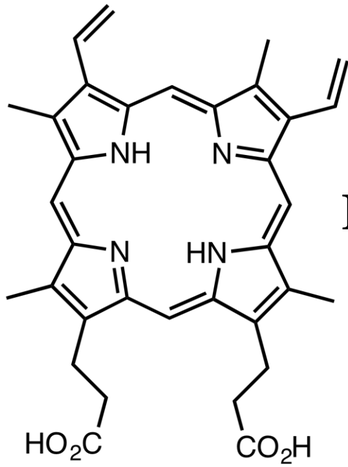


PpIX - photoluminescent photodynamic therapy drug

Fluorescent cell images

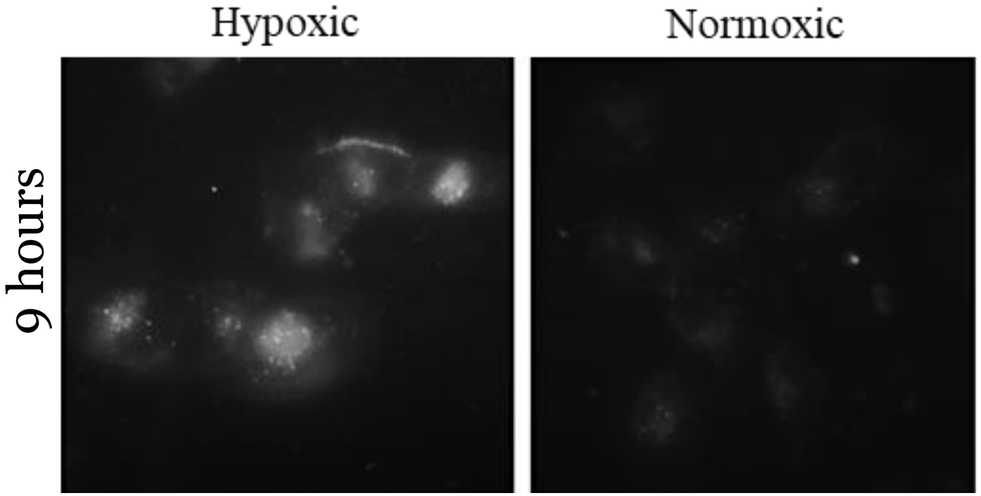


❖ **Successful demonstration of ROS triggered drug release.**

# Conclusion

- Hydrogen peroxide responsive theranostic nanoplatform with tunable emission wavelength accompanied by a “turn on” $^{19}F$ MRI, chemiluminescence signal and drugs release was developed.
- The nanoparticle exhibited 560-fold chemiluminescence signal enhancement within 0.1 minutes after addition of hydrogen peroxide.
- Ratiometric imaging of $^{19}F$ NMR was also realized with 19-fold signal enhancement, which shows strong potential for $^{19}F$ MRI imaging.
- Further optimizations will be explored to reveal the ultrasound imaging potential of the nanoparticles.

# Reference List


[1] M. C. Boonstra, S. W. L. De Geus, H. A. J. M. Prevoo, L. J. A. C. Hawinkels, C. J. H. Van De Velde, P. J. K. Kuppen, A. L. Vahrmeijer, and C. F. M. Sier, “Selecting targets for tumor imaging: An overview of cancer-associated membrane proteins,” Biomarkers in Cancer, vol. 8, 2016.
[2] R. H. Fang, W. Gao, and L. Zhang, “Targeting drugs to tumours using cell membrane-coated nanoparticles,” Nature Reviews Clinical Oncology, vol. 20, no. 1, pp. 33–48, 2022.
[3] S. T. Barry, D. I. Gabrilovich, O. J. Sansom, A. D. Campbell, and J. P. Morton, “Therapeutic targeting of tumour myeloid cells,” Nature Reviews Cancer, vol. 23, no. 4, pp. 216–237, 2023.
[4] W. Yi, P. Xiao, X. Liu, Z. Zhao, X. Sun, J. Wang, L. Zhou, G. Wang, H. Cao, D. Wang, and Y. Li, “Recent advances in developing active targeting and multi-functional drug delivery systems via bioorthogonal chemistry,” Signal Transduction and Targeted Therapy, vol. 7, no. 1, 2022.
[5] H. Sies, V. V. Belousov, N. S. Chandel, M. J. Davies, D. P. Jones, G. E. Mann, M. P. Murphy, M. Yamamoto, and C. Winterbourn, “Defining roles of specific reactive oxygen species (ROS) in cell biology and physiology,” Nature Reviews Molecular Cell Biology, vol. 23, no. 7, pp. 499–515, 2022.
[6] E. R. Brannon, M. V. Guevara, N. J. Pacifici, J. K. Lee, J. S. Lewis, and O. Eniola-Adefeso, “Polymeric particle-based therapies for acute inflammatory diseases,” Nature Reviews Materials, vol. 7, no. 10, pp. 796–813, 2022.
[7] Z. Tu, Y. Zhong, H. Hu, D. Shao, R. Haag, M. Schirner, J. Lee, B. Sullenger, and K. W. Leong, “Design of therapeutic biomaterials to control inflammation,” Nature Reviews Materials, vol. 7, no. 7, pp. 557–574, 2022.
[8] A. M. Garcia-Campana and W. R. G. Baeyens, “Mechanism and Application of Peroxyoxalate Chemiluminescence,” in Chemiluminescence in Analytical Chemistry, New York: Marcel Dekker, Inc, 2001.
[9] A. Boaro and F. H. Bartoloni, “Peroxyoxalate high-energy intermediate is efficiently decomposed by the catalyst imidazole,” Photochemistry and Photobiology, vol. 92, no. 4, pp. 546–551, 2016.
[10] E. C. Cheung and K. H. Vousden, “The role of ROS in tumour development and progression,” Nature Reviews Cancer, vol. 22, no. 5, pp. 280–297, 2022.
[11] C. Andreou, R. Weissleder, and M. F. Kircher, “Multiplexed imaging in oncology,” Nature Biomedical Engineering, vol. 6, no. 5, pp. 527–540, 2022.
[12] G. Saravanakumar, J. Kim, and W. J. Kim, “Reactive-oxygen-species-responsive drug delivery systems: Promises and challenges,” Advanced Science, vol. 4, no. 1, p. 1600124, 2016.
[13] Y. Yang and F. Zhang, “Activatable chemiluminescent molecular probes for Bioimaging and Biosensing,” Analysis & Sensing, vol. 1, no. 2, pp. 75–89, 2021.
[14] P. Cheng and K. Pu, “Molecular imaging and disease theranostics with renal-clearable optical agents,” Nature Reviews Materials, vol. 6, no. 12, pp. 1095–1113, 2021.
[15] Y. Yang and F. Zhang, “Activatable chemiluminescent molecular probes for Bioimaging and Biosensing,” Analysis & Sensing, vol. 1, no. 2, pp. 75–89, 2021.
[16] J. B. Grimm and L. D. Lavis, “Caveat fluorophore: An insiders’ guide to small-molecule fluorescent labels,” Nature Methods, vol. 19, no. 2, pp. 149–158, 2021.
[17] Z. Wang, J. Huang, J. Huang, B. Yu, K. Pu, and F. J. Xu, “Chemiluminescence: From mechanism to applications in biological imaging and therapy,” Aggregate, vol. 2, no. 6, 2021.
[18] J. Huang and K. Pu, “Activatable molecular probes for second near-infrared fluorescence, chemiluminescence, and photoacoustic imaging” Angewandte Chemie, vol. 132, no. 29, pp. 11813–11827, 2020.
[19] J. Huang, J. Li, Y. Lyu, Q. Miao, and K. Pu, “Molecular optical imaging probes for early diagnosis of drug-induced acute kidney injury,” Nature Materials, vol. 18, no. 10, pp. 1133–1143, 2019.
[20] D. Cui, J. Li, X. Zhao, K. Pu, and R. Zhang, “Semiconducting polymer nanoreporters for near-infrared chemiluminescence imaging of immunoactivation,” Advanced Materials, vol. 32, no. 6, p. 1906314, 2019.

# Reference List


[21] S. Ye, N. Hananya, O. Green, H. Chen, A. Q. Zhao, J. Shen, D. Shabat, and D. Yang, “A highly selective and sensitive chemiluminescent probe for real-time monitoring of hydrogen peroxide in cells and animals,” Angewandte Chemie International Edition, vol. 59, no. 34, pp. 14326–14330, 2020.
[22] J. Chen, L. Chen, Y. Wu, Y. Fang, F. Zeng, S. Wu, and Y. Zhao, “A H2O2-activatable nanoprobe for diagnosing interstitial cystitis and liver ischemia-reperfusion injury via multispectral optoacoustic tomography and NIR-II Fluorescent Imaging,” Nature Communications, vol. 12, no. 1, 2021.
[23] P. Sun, F. Qu, C. Zhang, P. Cheng, X. Li, Q. Shen, D. Li, and Q. Fan, “Nir-II excitation Phototheranostic platform for synergistic photothermal therapy/chemotherapy/chemodynamic therapy of breast cancer bone metastases,” Advanced Science, vol. 9, no. 33, p. 2204718, 2022.
[24] X. Yan, W. Lin, H. Liu, W. Pu, J. Li, P. Wu, J. Ding, G. Luo, and J. Zhang, “Wavelength-tunable, long lifetime, and biocompatible luminescent nanoparticles based on a vitamin e-derived material for inflammation and tumor imaging,” Small, vol. 17, no. 25, p. 2100045, 2021.
[25] J. Jeon, D. G. You, W. Um, J. Lee, C. H. Kim, S. Shin, S. Kwon, and J. H. Park, “Chemiluminescence resonance energy transfer–based nanoparticles for quantum yield–enhanced cancer phototheranostics,” Science Advances, vol. 6, no. 21, 2020.
[26] J. Jeon, B. Yoon, S. H. Song, W. Um, Y. Song, J. Lee, D. G. You, J. Y. An, and J. H. Park, “Chemiluminescence resonance energy transfer-based immunostimulatory nanoparticles for sonoimmunotherapy,” Biomaterials, vol. 283, p. 121466, 2022.
[27] J. Ding, G. Lu, W. Nie, L. L. Huang, Y. Zhang, W. Fan, G. Wu, H. Liu, and H. Y. Xie, “Self-activatable photo-extracellular vesicle for synergistic trimodal anticancer therapy,” Advanced Materials, vol. 33, no. 7, p. 2005562, 2021.
[28] Y. C. Chen, Y. J. Liu, C. L. Lee, K. Y. Pham, D. Manoharan, S. Thangudu, C. H. Su, and C. S. Yeh, “Engineering H2O2 and O2 self-supplying nanoreactor to conduct synergistic chemiexcited photodynamic and calcium-overloaded therapy in orthotopic hepatic tumors,” Advanced Healthcare Materials, vol. 11, no. 20, 2022.
[29] L. Wu, Y. Ishigaki, W. Zeng, T. Harimoto, B. Yin, Y. Chen, S. Liao, Y. Liu, Y. Sun, X. Zhang, Y. Liu, Y. Liang, P. Sun, T. Suzuki, G. Song, Q. Fan, and D. Ye, “Generation of hydroxyl radical-activatable ratiometric near-infrared bimodal probes for early monitoring of tumor response to therapy,” Nature Communications, vol. 12, no. 1, 2021.
[30] L. Su, Y. Chen, H. Huo, N. Liao, Y. Wu, X. Ge, Z. Guo, Z. Chen, X. Zhang, and J. Song, “Nir-II ratiometric chemiluminescent/fluorescent reporters for real-time monitoring and evaluating cancer photodynamic therapy efficacy,” Small, vol. 18, no. 41, p. 2202551, 2022.
[31] D. Taherinia and A. Fattahi, “Inducing high exo selectivity in Diels–Alder reaction by Dimethylborane Substituent: A DFT study,” Scientific Reports, vol. 12, no. 1, 2022.
[32] R. LeSar, Introduction to computational materials science: Fundamentals to applications. Cambridge: Cambridge University Press, 2016.
[33] Gaussian 16, Revision C.01, J. Frisch, W. Trucks, B. Schlegel, E. Scuseria, Gaussian, Inc., Wallingford CT, 2016.
[34] Y.-H. Lin, H.-M. Chang, F.-P. Chang, C.-R. Shen, C.-L. Liu, W.-Y. Mao, C.-C. Lin, H.-S. Lee, and C.-N. Shen, “Protoporphyrin IX accumulation disrupts mitochondrial dynamics and function in ABCG2-deficient hepatocytes,” FEBS Letters, vol. 587, no. 19, pp. 3202–3209, 2013.